WATERSHED SCIENCE BULLETIN

Center for Watershed Protection Association

Journal of the Center for Watershed Protection Association

Monitoring Stream Restoration in Howard County, Maryland to Determine Effectiveness in Reducing Pollutant Loads

Colin R. Hill,[a*] Michael J. Pieper,[b] William Medina,[c] and Mark S. Richmond[d]

Watershed Science Bulletin is a publication of the Center for Watershed Protection Association

"*Monitoring Stream Restoration in Howard County, Maryland to Determine Effectiveness in Reducing Pollutant Loads* " was first published in the *Watershed Science Bulletin* April 2019.

Front cover photo courtesy of Seth Dellinger, KCI Technologies.

Monitoring Stream Restoration in Howard County, Maryland to Determine Effectiveness in Reducing Pollutant Loads

Colin R. Hill,[a] Michael J. Pieper,[b] William Medina,[c] and Mark S. Richmond[d]*

[a] *Senior Project Scientist, KCI Technologies, Sparks, MD, colin.hill@kci.com*

[b] *Senior Project Manager, KCI Technologies, Sparks, MD*

[c] *Project Engineer, KCI Technologies, Sparks, MD*

[d] *Stormwater Management Division Chief, Howard County Department of Public Works, Columbia, MD*

[*] *Corresponding author.*

Abstract

Under the 2010 Chesapeake and Atlantic Coastal Bays Trust Fund program, the Howard County Department of Public Works initiated a monitoring program at the Brampton Hills stream restoration project site located in Ellicott City, Maryland to evaluate the effectiveness of stream restoration in reducing loading of primary pollutants nitrogen, phosphorus, and sediment. Monitoring efforts included water quality sampling, both baseflow and storm flow, for two years prior to restoration (2010–2011) and for six years post-restoration (2012–2017). We developed a procedure using precipitation data to derive modeled storm flows using the U.S. Environmental Protection Agency's Storm Water Management Model, calibrated using verified gaged flow data, as well as derived base-flows, to create an annual flow record at five-minute intervals, enabling estimates of annual loading rates for total nitrogen (TN), total phosphorus (TP), and total suspended solids (TSS). We calculated pollutant loads using the U.S. Army Corps of Engineers FLUX32 load estimation software for each sampling parameter and compared pre- and post-restoration loading rates to obtain estimates of load reductions resulting from the project. We then standardized loads by flow volume to allow for more direct comparisons since total annual flows differed considerably from year to year during the period of study. We calculated reduction rates per linear foot of restored stream of 0.20 pounds per foot per year (lbs/ft/yr) for TN, 0.20 lbs/ft/yr for TP and 73.4 lbs/ft/yr for TSS. Overall, the study found that the stream restoration project led to a considerable reduction of nutrients and suspended solids being generated within the study area.

Introduction

In 2009, the Howard County Department of Public Works received grant funding through the 2010 Chesapeake and Atlantic Coastal Bays Trust Fund's Local Implementation Grant program for Little Patuxent River watershed restoration. A component of the grant program is an evaluation of the effectiveness of implemented restoration projects and strategies and the tracking of progress toward meeting the overall watershed restoration goals. Following guidance provided in the *2010 Trust Fund Water Quality Monitoring Strategy* (Trust Fund Evaluation Workgroup 2009) and the Water Environment Research Foundation's *Urban Stormwater BMP Performance Monitoring Manual* (Geosyntec Consultants and Wright Water Engineers, Inc. 2009), a monitoring program was developed and initiated to evaluate the effectiveness of restoration efforts proposed within the Red Hill Branch subwatershed. After consultation with Howard County and the Maryland Department of Natural Resources (DNR), KCI Technologies, Inc. recommended that the primary monitoring approach be project-specific monitoring to demonstrate the effectiveness of stream restoration in reducing loading of primary pollutants nitrogen, phosphorus, and sediment. Schueler and Stack (2014) note that origins of the Chesapeake Bay Program (CBP)-approved pollutant loading rates for urban stream restoration were based on a single study conducted in Baltimore County, Maryland (Stewart 2008) due to a lack of relevant studies on nutrient reductions associated with urban stream restoration. The current CBP rates are based on six unpublished studies on urban stream erosion rates in Maryland and southeastern Pennsylvania (Schueler and Stack 2014); therefore, a need to evaluate nutrient reduction rates for this specific project was identified.

The Brampton Hills stream restoration project offered a good case study opportunity given that the project was in the design phase and planned for construction in the 2010–2011 time frame, which would provide adequate time to initiate the monitoring strategy and collect approximately one to two years of pre-restoration baseline data. We developed the monitoring strategy in summer of 2009 to ensure that adequate baseline data were collected. This study evaluated the effectiveness of the Brampton Hills stream restoration project—which included bed and bank stabilization efforts for approximately 3,165 linear feet of stream channel in addition to outfall stabilization—by comparing the pollutant loads before and after restoration activities.

The stream restoration project involved the stabilization of an approximate 2,100-linear foot segment of an unnamed tributary to the Red Hill Branch located immediately downstream of a stormwater outfall adjacent to Middlesmoor Court, as well as an additional 300 feet of outfall stabilization. The project reach is a first-order stream located in an urbanized landscape with predominantly residential land use. The stream channel was likely adjusting to increased surface flows by incising or down cutting. Overall, the pre-restoration project reach was relatively narrow in the upper portion, becoming increasingly wider downstream but with no apparent floodplain connectivity. Restoration activities involved re-grading the stream bed and banks, using stone toe protection, applying bioenhancement techniques, installing imbricated riprap for bank protection, installing grade control structures, and providing soil stabilization to the banks and riparian area via a comprehensive planting plan that included live stakes, trees, shrubs, and various seeding mixtures. Additionally, a concurrent project was completed to repair an eroding drainage ditch that was contributing

Figure 1. Photographs representing pre-restoration conditions.

Figure 2. Photographs representing post-restoration conditions.

flow and pollutants from westbound Maryland Route 100 to the restoration reach. This project included re-grading and rip-rap armoring along approximately 765 linear feet of the ditch and installing a new storm drain pipe and manhole to convey water down a steep slope. The overall length of restored channel and outfalls totaled 3,165 linear feet for this project. Representative site photos showing pre- and post-restoration conditions are included in Figures 1 and 2, respectively.

The study design utilized a Before-After-Control-Impact approach (Green 1979) to compare pre-construction conditions to post-construction restoration conditions. A paired watershed approach was not selected due to budget constraints that could not support this level of long-term monitoring at an additional sampling location. Monitoring protocols for the Red Hill Branch subwatershed were developed to evaluate the existing water quality conditions and measure changes over time (i.e., pollutant load reductions) that can be directly attributed to restoration activities. Continuous flow data for the pre-restoration monitoring period were deemed unreliable after rigorous quality assurance/quality control (QA/QC) inspection. As a result, we developed a Storm Water Management Model (SWMM) to model stream discharge for two locations coinciding with existing water quality monitoring stations to allow for load calculations. Two versions of the model were developed to represent the hydrologic and hydraulic conditions before and after restoration to ensure consistency between pre- and post-construction load estimates.

Study Site

The study area is located within the Red Hill Branch subwatershed in central Howard County (Figure 3). The restoration reach is located on a first-order, unnamed tributary to the Red Hill Branch between Bramhope Lane and Maryland Route 100 and contains two monitoring sites, BH01 and BH02 (Figure 4). BH01 is the upstream site that characterizes water quality entering the restored stream reach (i.e., control site) and represents a 26.5 acre drainage area with approximately 25% impervious surface. BH02 is the downstream site that characterizes water quality exiting the stream reach (i.e., impact site) and represents a 57 acre drainage area with approximately 31% impervious surface. Due to study limitations, we were unable to monitor all inputs to the stream reach, including three stormdrain outfalls and the drainage ditch from Maryland Route 100.

Methods

Water Quality Sampling

Field crews collected water quality samples using manual and automated sampling techniques following a modification of standard practice described by Stenstrom and Strecker (1993). Crews manually collected baseflow grab samples from each monitoring station after a minimum of 72 hours of dry weather. Prior to 2011, field crews collected all storm flow samples manually. Manual sampling involved collecting a total of three discrete samples representing the rising limb, peak, and falling limb of the storm hydrograph from each station. Personnel

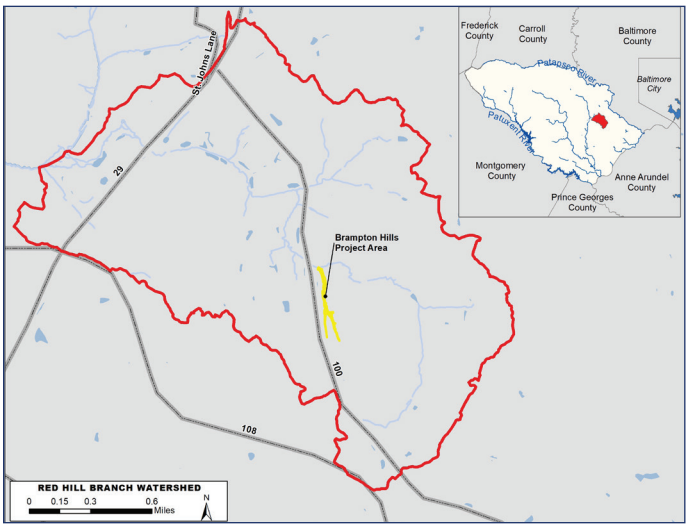

Figure 3. Site vicinity map.

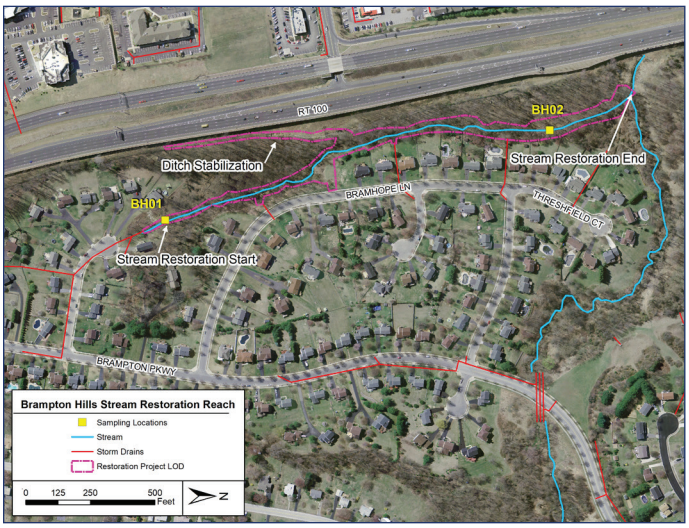

Figure 4. Brampton Hills monitoring locations.

recorded stage measurements approximately every 10 minutes and generated by hand a hydrograph that was used to identify the appropriate time for collecting the peak and falling limb samples. Samples were preserved on ice, sent to a laboratory certified by National Environmental Laboratory Accreditation Program, and analyzed for the following parameters: total phosphorus (TP), total nitrogen (TN; the sum of total Kjeldahl nitrogen, nitrate, and nitrite), and total suspended solids (TSS).

Beginning in 2012, field crews began collecting storm flow samples using ISCO 6712 full-size automated samplers due to a change in consultant collecting the samples. Crews deployed samplers at secure locations corresponding to the monitoring stations described above, and each sampler was stocked with ice to preserve samples. Bubbler flow modules were attached to the automated samplers to log stage and determine discrete bottle position relative to the storm hydrograph. Crews selected bottles that most closely matched rising, peak, and falling limb conditions and combined them into composite samples representing each separate limb before transporting them to the laboratory.

Flow Monitoring

The Maryland DNR performed pre-restoration flow monitoring using pressure transducer data loggers to record water level at five-minute intervals and developed rating curves at established cross sections by converting stage to discharge. However, after extensive QA/QC checks on pre-restoration flow data, this method was determined to be unreliable for calculating loads during this period due to changes in channel cross-section and inaccurate flow meter readings. To improve the quality of the flow data, DNR installed 90-degree v-notch weir structures within the channel at both the upstream and downstream monitoring locations following completion of restoration activities in early 2012. DNR installed pressure transducer data loggers to record water level at five-minute intervals and developed rating curves for each location by converting stage to discharge. They continuously monitored flow throughout the remainder of 2012 and continuing through 2017.

Discharge Modeling

The U.S. Environmental Protection Agency's SWMM, a dynamic simulation model for hydrology and hydraulics, was used to model stormwater runoff and streamflow to both sampling locations. The SWMM is a widely used tool for urban drainage design and planning, with hundreds of peer-reviewed articles and conference proceedings that describe the various applications of SWMM (Niazi et al. 2017). Two SWMM models were used for the analysis, one that represented the pre-restoration condition, and one that

Table 1. Number of wet weather event and base flow samples collected.

	Year	Number of Wet Weather Event Samples	Number of Baseflow Samples
Pre-Restoration Period	2010	8	8
	2011	8	8
	Total Pre-Restoration	16	16
Post-Restoration Period	2012	8	7
	2013	8	7
	2014	8	6
	2015	6	3
	2016	7	2
	2017	10	5
	Total Post-Restoration	47	30

Table 2. SWMM subcatchment input parameters.

Input Parameter	Description	Source
Evaporation	Dry weather evaporation rate	NOAA Technical Report NWS 84 (1982)
Area	Area	GIS analysis
%Imperv	Percent impervious	GIS analysis
Width	Runoff timing factor	Calculated from subcatchment geometry (modified in calibration)
%Slope	Surface slope	GIS analysis
Manning's n	Surface roughness	Default value (modified in calibration)
Depression storage	Interception	Default value (modified in calibration)
Curve number	TR-55 analysis	GIS analysis (modified in calibration)

represents the post-restoration condition with updates to the model each year to reflect changes in the watershed and stream channel.

SWMM estimates flows from balancing water volumes. Evapotranspiration, depression storage, and infiltration are subtracted from precipitation to estimate the direct runoff. SWMM's hydrologic calculations are based on several parameters that affect the volume and flow rate of stormwater runoff, calculated for six subcatchments delineated within the site drainage area to derive flows to each monitoring location. GIS layers representing subcatchments, land cover, and soil type were intersected to obtain an area average of the parameters describing the physical condition of the subcatchments. We then modeled runoff for each subcatchment using the following parameters, with source shown, presented in Table 2.

We also modeled the conveyances and channels in the watershed in SWMM to simulate water surface elevations. In this process, the discharge modeled in the subcatchment runoff model is routed through the receiving channel. The model uses dynamic flow calculations, which are capable of simulating backwater condition and surcharges. The parameters used for this model are based on the type of structure or channel: junctions, pipes, or natural channels. For this model, only natural channels were modeled, with junctions added at each significant change in channel dimension and geometry to distinguish them. Input parameters and associated sources are shown in Table 3.

Field crews performed surveys of the restoration site on an annual basis from the pre-restoration period and through the post-restoration period. The surveys include longitudinal profiles of the channel thalweg to derive channel slope and length, cross-sections at representative locations throughout

Table 3. SWMM channel input parameters.

Input Parameter	Description	Source
Outfall elevations	Invert	As-built survey
Junction elevations	Invert, top	As-built survey
Channel length	Thalweg length	Field survey
Channel shape	Rectangular, trapezoid, natural	Field survey
Channel roughness	Manning's n	Field survey
Channel cross-section	Cross-section dimensions	Field survey

the reach to derive channel shape, and weighted proportional pebble counts to determine channel roughness. We estimated roughness in the overbank area from field observations of vegetative cover. Each year as the model is updated, the most recent survey data representing channel slope, cross-section geometry, and channel/overbank roughness values are checked and updated where necessary to ensure that the current year's model reflects the conditions in the watershed.

The study obtained rainfall data primarily from the Meadowbrook Park rain gage, which is located approximately 0.8 miles northwest of the project site. The Meadowbrook Park data were occasionally missing records when the unit lost power or was taken offline for maintenance and repair. For the missing periods, we supplemented rainfall data with rainfall records from the rain gages at Centennial Park or Ellicott City that are part of the county's Contrail® OneRain monitoring system.

We calibrated the initial pre- and post-restoration models based on the post-restoration flow record following methods described in Rossman (2015) and James (2005). The model was calibrated primarily to match volume parameters as the annual volumes are the most critical factor in the annual load calculations. Model elements modified in the calibration process included subcatchment width, roughness coefficient and depression storage, infiltration parameters, and the time step. We then validated the model against additional flow records. Each year as the model was updated, it was checked against the measured flow record to ensure a basic level of consistency with measured data.

Base Flow Estimation for the Pre-Restoration Period

Due to the lack of gaged flow data, we had to estimate baseflow data for the pre-restoration period (2010–2011), as well as the first half of 2012. Beginning in June 2012, when the weirs and data loggers were installed, we derived baseflow values from the gaged flow records. For the ungaged period, we analyzed flow records from 2013 since that was the only year for which complete discharge records were available at the time of this analysis. We independently analyzed flow data from the upper station (BH01) and lower station (BH02), and a mean baseflow and baseflow index, which is the proportion of measured flow that can be attributed to baseflow, was obtained for each station.

Little information exists in the literature to estimate baseflows in small catchments. We attempted to use the U.S. Geological Survey's PART software (Rutledge 2007), but because of the small drainage area (<1.0 square miles) and the limited time period of the data, baseflow estimations for a shorter timeframe (e.g., months, quarters) would be less reliable. Consequently, an additional method was selected to estimate seasonal baseflows using the field-measured data from the second half of 2012 and all of 2013. Our method allowed us to mimic the seasonal variation that we had observed in the gaged record versus using a single annual baseflow record. The baseflow estimation procedure consisted of three steps that are outlined below.

1. Determine seasonal baseflows using the available field measured data.
2. Adjust baseflow estimates based on seasonal rainfall records to determine seasonal adjusted baseline flows.
3. Adjust baseline values to reflect seasonal precipitation conditions and obtain final estimated baseflow values.

The study partitioned flow records for each season beginning with summer 2012 and continuing through fall 2015. Within each season, flow records were analyzed using frequency distributions to segregate baseflows from storm flows. We then calculated seasonal baseflows using weighted averages of the baseflow records for each given time period (Table 4).

Since differences in gaged seasonal baseflows were observed between the years, we made adjustments based on seasonal rainfall records to determine normalized baseflow estimates to apply to the ungaged pre-restoration period. The study used seasonal rainfall records from the National Oceanic and Atmospheric Administration (NOAA) for the Baltimore/Washington International Thurgood Marshall (BWI) Airport in Linthicum, Maryland. We compared measured rainfall records for each season to long-term average rainfall records dating back to 1871 (141 years) to determine the deviation from normal precipitation (Table 5). In addition to the absolute rain differential (in inches), the percent increase from normal was calculated and a corresponding status was determined (i.e., normal, above average, below average). Deviations of less than 10% were considered "normal," and only deviations exceeding 10% percent were considered above (or below) normal.

Table 4. Seasonal gaged baseflows (cubic feet per second) based on weighted averages.

Station	Season	2012	2013	2014	2015	2016	2017
BH-01	Winter	n/a	0.027	0.037	0.030	0.045	0.022
BH-02	Winter	n/a	0.028	0.037	0.038	0.055	0.031
BH-01	Spring	n/a	0.028	0.044	0.027	0.038	0.023
BH-02	Spring	n/a	0.040	0.057	0.039	0.059	0.049
BH-01	Summer	0.012	0.021	0.023	0.022	0.029	0.024
BH-02	Summer	0.017	0.022	0.027	0.026	0.037	0.036
BH-01	Fall	0.016	0.019	0.019	0.019	0.023	0.027
BH-02	Fall	0.022	0.019	0.019	0.020	0.027	0.028

n/a indicates data not available

Table 5. Comparison of seasonal rainfall at BWI airport (NOAA 2014).

Year	Season	Average Rainfall (in.)	Measured Rainfall (in.)	Differential (in.)	Increase from Avg	Status
2010	Winter	9.32	14.45	5.13	55%	Above Avg
	Spring	11.08	11.22	0.14	1%	Normal
	Summer	10.82	10.65	-0.17	-2%	Normal
	Fall	10.66	13.25	2.59	24%	Above Avg
2011	Winter	9.32	7.31	-2.01	-22%	Below Avg
	Spring	11.08	10.93	-0.15	-1%	Normal
	Summer	10.82	16.66	5.84	54%	Above Avg
	Fall	10.66	19.08	8.42	79%	Above Avg
2012	Winter	9.32	9.46	0.14	2%	Normal
	Spring	11.08	5.74	-5.34	-48%	Below Avg
	Summer	10.82	11.77	0.95	9%	Normal
	Fall	10.66	11.84	1.18	11%	Above Avg
2013	Winter	9.32	8.7	-0.62	-7%	Normal
	Spring	11.08	8.27	-2.81	-25%	Below Avg
	Summer	10.82	11.71	0.89	8%	Normal
	Fall	10.66	12.09	1.43	13%	Above Avg

We examined seasonal differences in the 2012–2013 data set to determine whether any patterns exist between abnormal rainfall and resulting baseflows. Lower baseflows were often observed during seasons with lower than average precipitation, and conversely, higher baseflows generally were observed during periods of above-average precipitation. To account for likely reductions in baseflow due to rainfall patterns, we developed a correction factor to establish baseline seasonal baseflows using the 2012–2013 gaged flow data. The original weighted averages for the 2013 winter and 2013 summer seasons, when rainfall was considered to be "normal," were used to establish baseline values for these two seasons. Spring 2013 was considered "below average," thus a correction factor was applied to estimate the typical seasonal baseflow. A comparison of gaged baseflow and BWI airport rainfall data from 2012–2014 found a linear relationship between seasonal rainfall and seasonal baseflows; therefore, the inverse of the percentage of deviation from normal rainfall was applied as a percentage of additional baseflow. Adjusted seasonal baseflow values are shown in Table 6.

Table 6. Adjusted seasonal baseflows.

Season	BH02	BH01
	Adjusted Baseline	Adjusted Baseline
	(cfs)	(cfs)
Winter	0.028	0.027
Spring	0.040	0.035
Summer	0.022	0.021
Fall	0.021	0.018
Average	0.028	0.025

The study applied the seasonal adjusted flow values to the respective seasons in 2010, 2011, and the first half of 2012 as the baseline flow values. We adjusted the baseline values upward or downward for seasons with above average or below average rainfall, respectively, to obtain estimated baseflow values. Estimated seasonal baseflow values are shown in Table 7.

Table 7. Estimated seasonal baseflows.

Year	Season	BH02		BH01	
		Baseline Value	Estimated Baseflow	Baseline Value	Estimated Baseflow
		(cfs)	(cfs)	(cfs)	(cfs)
2010	Winter	0.028	0.040	0.027	0.040
	Spring	0.040	0.040	0.035	0.035
	Summer	0.022	0.020	0.021	0.017
	Fall	0.021	0.026	0.018	0.022
2011	Winter	0.028	0.022	0.027	0.021
	Spring	0.040	0.040	0.035	0.035
	Summer	0.022	0.034	0.021	0.032
	Fall	0.021	0.038	0.018	0.032
2012	Winter	0.028	0.028	0.027	0.027
	Spring	0.040	0.021	0.035	0.018

Event Mean Concentration and Load Calculations

The study calculated storm flow pollutant loads using event mean concentrations (EMCs) for each parameter and modeled storm flow discharges. An EMC is a statistical parameter used to represent the flow-proportional average concentration of a given parameter during a storm event (U.S. Environmental Protection Agency 2002). The EMC for a storm event where discrete samples have been collected (i.e. samples collected during the rise, peak, and falling limb of a storm event) was calculated using the following formula:

$$EMC = \frac{\sum_{i=1}^{n} V_i C_i}{\sum_{i=1}^{n} V_i}$$

where,

V: volume of flow during period i

C: average concentration associated with period i

n: total number of measurements taken during event

We calculated flow volume for each flow measurement interval by taking the average discharge between the start of the period and the end of the period and multiplying by the number of seconds in the interval (i.e., 300 seconds in a 5-minute interval). We then plotted discharge data graphically to produce hydrographs, which were used to partition out storm flow from baseflow and to separate the rising, peak, and falling limb segments of each storm event. The flow volume for each measurement interval was summed for each limb to determine the volume of flow attributed to each limb sampled. Storm flow was separated from baseflow, typically when discharge decreased to a value equal to 1.1 times the baseflow discharge prior to the storm event. However, when these criteria could not be applied due to atypical conditions, the following alternative criteria were utilized:

1. If no additional precipitation occurred and 1.1 times the baseflow conditions did not return, the storm flow was cut 24 hours after precipitation stopped.
2. If additional precipitation occurred (i.e., a new storm event) after precipitation stopped and the falling limb sample was collected, the storm flow was cut prior to the new storm event regardless of discharge.

We calculated annual loads for TN, TP, and TSS using the U.S. Army Corps of Engineers' FLUX32 load estimation software (Walker 1999). This model uses a variety of calculation techniques to estimate the average mass discharge or loading from a given tributary based on continuous flow data and laboratory-analyzed grab sample concentrations. We input the mean daily discharges that were derived from the SWMM model to calculate annual loading rates. EMCs representing pollutant concentrations throughout a storm event were paired with average event discharges when input into FLUX32. The program calculates loads using six methods, and method applicability generally depends on the relationship between concentration and flow (i.e., C/Q relationship). Because the C/Q relationship differed between the pre- and post-restoration sampling periods, we selected different methods for calculating the load estimates for each period. We selected the methods that minimized the coefficient of variation (CV) or error in the loading estimates while also maintaining the ability to compare the pre- and post-restoration loading estimates without introducing bias.

We calculated annual loads for the pre-restoration period (2010–2011) using the second order regression method (Walker 1987) because a fairly strong C/Q relationship was observed for each of the parameters. This method adjusts the flow-weighted mean concentration for differences between the average sampled flow and the average total flow using the C/Q slope with an adjustment factor to account for differences in variance between the sampled and total flow distributions (Walker 1987). We calculated annual loads for the post-restoration period (2012–2017) using the flow-weighted concentration (ratio estimate) method (Walker 1999) due to weak C/Q relationships for all parameters. This method bases the loading estimate on the flow-weighted average concentration times the mean flow over the averaging period, which amounts to a "ratio estimate" according to classical sampling theory. Flow-weighted average concentrations are concentrations that are adjusted for the variability in stream flow over a given period of time (e.g., monthly or annually).

We combined sample and flow data from 2010 and 2011 to obtain pre-restoration loading estimates for each site. Prior to running the model, we stratified flow data into three strata since the relationship between concentration and discharge can differ greatly between samples types. The low-flow strata

Table 8. Pre-Restoration Loading Estimates (2010–2011).

Site	Total Nitrogen			Total Phosphorus			Total Suspended Solids		
	Loading Rate (lbs/y)	Flow-Weighted Conc. (mg/L)	CV*	Loading Rate (lbs/y)	Flow-Weighted Conc. (mg/L)	CV	Loading Rate (lbs/y)	Flow-Weighted Conc. (mg/L)	CV
BH01	495.5	3.00	0.05	55.0	0.33	0.10	8,113	49.1	0.26
BH02	1633.7	3.75	0.09	951.5	2.18	0.26	323,570	742	0.27

**Coefficient of variation*

Table 9. Post-restoration Loading Estimates (2012-2017).

Site	Total Nitrogen			Total Phosphorus			Total Suspended Solids		
	Loading Rate (lbs/y)	Flow-Weighted Conc. (mg/L)	CV*	Loading Rate (lbs/y)	Flow-Weighted Conc. (mg/L)	CV	Loading Rate (lbs/y)	Flow-Weighted Conc. (mg/L)	CV
BH01	368.9	2.64	0.04	33.3	0.24	0.08	2,611	18.7	0.12
BH02	535.0	1.85	0.04	60.2	0.21	0.09	8,504	30.8	0.19

**Coefficient of variation*

included all baseflow samples, while the storm flows were further stratified into a low- to moderate-storm-flow stratum and a high-flow stratum. This process was repeated using sample and flow data from 2012 through 2017 to obtain post-restoration loading estimates.

Results and Discussion

Pollutant Loads

We calculated EMCs for each storm event, as well as the average discharge (in cubic feet/second) that were used to calculate pollutant loads and flow-weighted concentrations for TN, TP, and TSS in FLUX32 for pre-restoration and post-restoration time periods, as shown in Tables 8 and 9, respectively. Comparisons of flow-weighted concentrations for TN, TP, and TSS are shown in Figures 5, 6, and 7, respectively.

Load Reductions

To allow for a more direct comparison of pollutant loads between pre- and post-restoration conditions, we standardized loading rates by flow volume (cubic feet) since

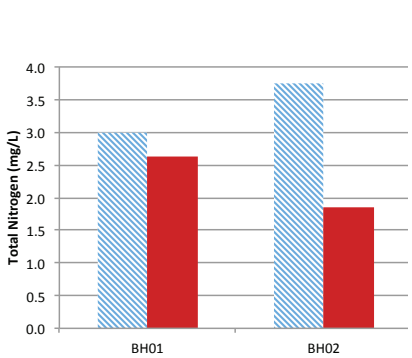

Figure 5. Comparison of flow-weighted concentrations for total nitrogen.

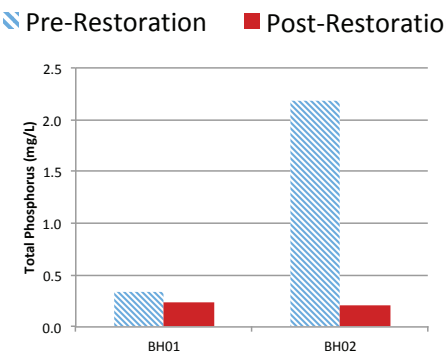

Figure 6. Comparison of flow-weighted concentrations for total phosphorus.

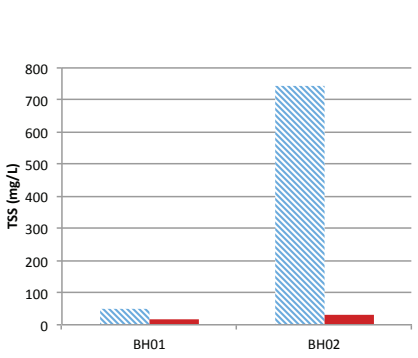

Figure 7. Comparison of flow-weighted concentrations for total suspended solids.

total annual flows differed considerably from year to year during the period of study and because flow volume is a major component of loading rate calculations[1]. This is a non-standard practice recommended by our peer reviewers at the Maryland DNR to offset climatic variability between the pre- and post-restoration period. We experienced substantial differences in rainfall during our pre-restoration period, which included Hurricane Irene and Tropical Storm Lee, followed by a few abnormally dry years in the post-restoration period. Therefore, we applied a corrective factor to balance the flow volumes between periods using average annual flow volumes during the period of study.

We calculated standardized loads for both the pre- and post-restoration periods by multiplying the loading rate (lbs/year) by the number of years in the monitoring period to obtain a periodic load (in lbs), then dividing by the total volume of flow modeled for that that time period (periodic volume) in cubic feet. We then multiplied the standardized loading rate (in lbs/cubic foot) by the average annual flow volume determined from the eight years of record (i.e., 2010–2017) to obtain a standardized annual load for each site.

The study calculated the estimated load reductions as the difference between the pre-restoration standardized loads and post-restoration standardized loads at the downstream site (BH02). We calculated the per linear foot load reduction by dividing the estimated load reduction by 3,165 linear feet of restored channel. Results of the estimated annual load reductions for TN, TP, and TSS are presented in Table 10, 11, and 12, respectively. We calculated an estimated reduction of nearly 619 lbs per year of TN, or approximately 0.20 lbs per linear foot of restored channel. TP showed an estimated reduction of nearly 644 lbs per year, or approximately 0.20 lbs per linear foot of restored channel. TSS showed an estimated reduction of more than 232,000 lbs per year following restoration, or approximately 73.4 lbs per linear foot of restored channel.

Comparing the ratios in loading rates and standardized loads between the upstream (BH01) and downstream (BH02) sites provides a good indication of the source reduction in nutrients and sediment that can be directly attributed to the stream restoration efforts. Pre-restoration standardized load ratios were high for both TP and TSS, indicating loads that were 15.7 times greater and 36.1 times greater downstream, respectively. TN was slightly better, with values 3.0 times greater at the downstream site. In contrast, post-restoration standardized load ratios ranged between 1.5 and 3.4 for all parameters. Similar trends were observed for the loading rate ratios. The percent difference in pre- and post- ratios for TN was 46% for loading rates and 39% for standardized loads. The percent difference was considerably larger for TP (85% and 83%) and TSS (86% and 86%), indicating a considerably greater reduction in TP and TSS loads.

Table 10. Estimated load reductions for total nitrogen.

	Total Nitrogen					
Site	**Loading Rate (lbs/y)**	**Periodic Load (lbs)**	**Periodic Volume (cf)**	**Standardized Load (lbs/cf)**	**Avg Volume per Year (cf)**	**Standardized Load (lbs)**
Pre-Restoration Estimates (2010–2011)						
BH01	495	990	5,285,795	0.000187	2,184,860	409
BH02	1,634	3,265	13,952,393	0.000234	5,219,567	1,221
Post-Restoration Estimates (2012–2017)						
BH01	369	2,214	12,193,085	0.000182	2,184,860	397
BH02	535	3,211	27,804,140	0.000115	5,219,567	603
					Est. Load Reduction (lbs)	619
					Reduction/LF restored (lbs)	0.20

[1]*English units are used in association with this work, as they are the customary tracking and reporting units in this subject.*

A comparison of standardized loading rates between pre- and post-restoration conditions showing the contribution of the upstream input (BH01) to the downstream output (BH02) is presented in Figures 8, 9, and 10 for TN, TP, and TSS, respectively. For all three parameters, a notable reduction in the output load can be observed between the pre- and post-restoration condition despite minor differences in the upstream loads at the control site (BH01) between periods.

Conclusions and Recommendations

The results of the loading calculations suggest the stream restoration effort led to a considerable reduction of nutrients and suspended solids being generated within the study area (e.g., stream bank and bed erosion) that support the use of stream restoration as a beneficial practice for pollutant reduction. These reductions can likely be attributed to decreases in localized bank erosion, which was previously a significant source of suspended solids, as well as increased floodplain reconnection and vegetation enhancement.

Some caveats regarding the use of SWMM for modeled flow and FLUX32 for loading estimates should be discussed, however. First, loads can be underestimated in small, flashy, urban streams when using the mean daily flow. The study reach occurs in such a setting, therefore, it is possible that loads are being underestimated. Secondly, Walker's (1999) eutrophication assessment and prediction models, such as those utilized in FLUX32, were initially developed for reservoirs and large tributaries to reservoirs. The use of FLUX32 for a small, flashy, first-order stream may add additional uncertainty in the overall loading estimates,

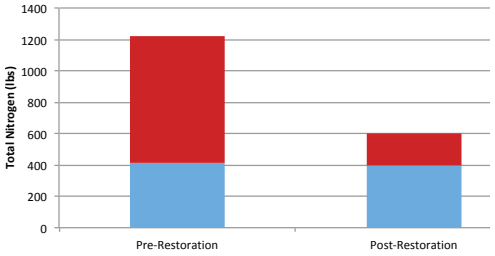

Figure 8. Comparison of standardized loads for total nitrogen.

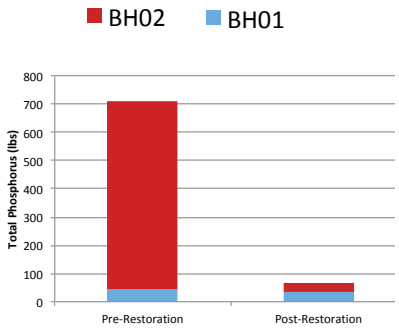

Figure 9. Comparison of standardized loads for total phosphorus.

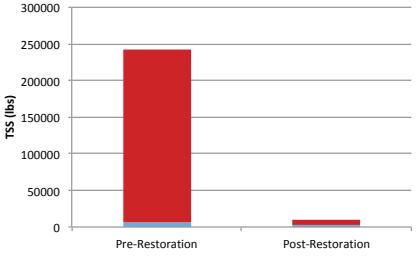

Figure 10. Comparison of standardized loads for total suspended solids.

Table 11. Estimated load reductions for total phosphorus.

	Total Phosphorus					
Site	Loading Rate (lbs/y)	Periodic Load (lbs)	Periodic Volume (cf)	Standardized Load (lbs/cf)	Avg Volume per Year (cf)	Standardized Load (lbs)
Pre-Restoration Estimates (2010–2011)						
BH01	55	109.95	5,285,795	0.0000208	2,184,860	45
BH02	951	1,902	13,952,393	0.0001363	5,219,567	711
Post-Restoration Estimates (2012–2017)						
BH01	33	200	12,193,085	0.000016	2,184,860	36
BH02	60	361	27,804,140	0.000013	5,219,567	68
					Est. Load Reduction (lbs)	644
					Reduction/LF restored (lbs)	0.20

Table 12. Estimated load reductions for total suspended solids.

Site	Total Suspended Solids					
	Loading Rate (lbs/y)	Periodic Load (lbs)	Periodic Volume (cf)	Standardized Load (lbs/cf)	Avg Volume per Year (cf)	Standardized Load (lbs)
Pre-Restoration Estimates (2010–2011)						
BH01	8,113	16,215	5,285,795	0.00307	2,184,860	6,702
BH02	323,570	646,696	13,952,393	0.04635	5,219,567	241,928
Post-Restoration Estimates (2012–2017)						
BH01	2,611	15,670	12,193,085	0.00129	2,184,860	2,808
BH02	8,504	51,014	27,804,140	0.00183	5,219,567	9,577
				Est. Load Reduction (lbs)		232,351
				Reduction/LF restored (lbs)		73.4

Table 13. Comparison of loading rates between upstream and downstream sampling locations.

Site	Total Nitrogen		Total Phosphorus		TSS	
	Loading Rate (lbs/y)	Standardized Load (lbs)	Loading Rate (lbs/y)	Standardized Load (lbs)	Loading Rate (lbs/y)	Standardized Load (lbs)
Pre-Restoration Estimates						
BH01	495	409	55.0	45	8,113	6,702
BH02	1,634	1,221	951.5	711	323,570	241,928
BH02:01 Ratio	3.3	3.0	17.3	15.7	39.9	36.1
Post-Restoration Estimates						
BH01	369	397	37	36	2,611	2,808
BH02	535	603	65	68	8,504	9,577
BH02:01 Ratio	1.5	1.5	1.8	1.9	3.3	3.4
Percent Difference Between Ratios	46%	39%	85%	83%	88%	86%

which could, in turn, influence the removal rates. Thirdly, CV estimates for pre-restoration loading estimates at BH02 were higher than expected due to the increased variability in EMCs observed at this location, likely arising from the actively eroding and degrading conditions occurring within the reach. This leads to an increased uncertainty in the loading estimates during this period, which could influence the removal rates. For this reason, we recommend obtaining an adequate number of pre-restoration samples to improve confidence. Finally, we observed a reduction in flow-weighted concentrations at our control site for all three parameters and attributed these differences to two factors. Installation of the upstream weir for gaging purposes resulted in backwater conditions that were not present previously, which may have resulted in more suspended solids settling out prior to sampling. Additionally, the smaller sample size during this period resulted in higher CV values, which were subsequently reduced in the post-restoration period as additional samples were collected and added to the data set. To compensate for these differences, we calculated load reductions two ways: one by subtracting the BH01 loads from the BH02 loads before comparing the pre- and post-restoration loads at BH02, and the other without the subtraction of BH01. We found that the effect of subtracting the BH01 loads was negligible on the overall load reduction per linear foot restored, and since this wasn't the only source of inputs to the restoration reach, we decided against this approach.

We continue to monitor the Brampton Hill stream restoration project and will revise the pollutant load reductions annually as future data become available. Because there are relatively few long-term studies evaluating the effectiveness of stream restoration projects in reducing pollutant loads, we recommend more projects be monitored to better define pollutant removal rates that can be used more broadly for both accounting purposes (i.e, waste load allocations) and to better inform stream restoration techniques and practices. Numerous factors can affect pollutant load reductions such as the extent and nature of prior stream erosion, physiographic setting, stream order, surrounding land use, and so forth, along with variations in stream restoration techniques, all of which highlights a need for more studies that capture some of these other variables to help cover a wider range of stream restoration projects.

References

Geosyntec Consultants and Wright Water Engineers, Inc. 2009. Urban stormwater BMP performance monitoring manual. Alexandria, VA: Water Environment Research Foundation.

Green, R. H. 1979. Sampling design and statistical methods for environmental biologists. Chichester, England: Wiley Interscience.

James, W. 2005. Rules for responsible modeling, 4th Edition. Guelph, Ontario, Canada: Computational Hydraulics International.

Niazi, M., C. Nietch, N. Jackson, B. Bennett, M. Maghrebi, M. Tryby, and A. Massoudieh. 2017. Storm Water Management Model (SWMM): Performance review and gap analysis. Journal of Sustainable Water in the Built Environment. 3(2):04017002 1-32.

National Oceanic and Atmospheric Administration. 2011. National Weather Service Forecast Office observed weather for Baltimore/Washington International Thurgood Marshall Airport, published online August 2011 and retrieved on July 17, 2014. Website no longer available.

National Oceanic and Atmospheric Administration. 1982. Mean monthly, seasonal and annual pan evaporation for the United States. NOAA Technical Report NWS 84. Washington, DC: National Oceanic and Atmospheric Administration National Weather Service.

Rossman, L.A. 2015. Storm Water Management Model user's manual version 5.1. EPA/600/R-14/413b. Cincinnati, OH: U.S. Environmental Protection Agency Office of Research and Development.

Schueler, T. and B. Stack. 2014. Recommendations of the expert panel to define removal rates for individual stream restoration projects. Ellicott, MD: Chesapeake Stormwater Network and Center for Watershed Protection.

Stenstrom, M.K. and E.W. Strecker. 1993. Assessment of storm drain sources of contaminants to Santa Monica Bay, Volume II: Review of water and wastewater sampling techniques with an emphasis on stormwater monitoring requirements. Los Angeles, CA: UCLA School of Engineering and Applied Science.

Stewart, S. 2008. Spring Branch subwatershed: Small watershed action plan. Towson, MD: Baltimore County Department of Environmental Protection and Resource Management.

Trust Fund Evaluation Workgroup. 2009. 2010 trust fund water quality monitoring strategy. Sponsored by the University of Maryland, Maryland Department of Natural Resources, and Maryland Department of the Environment.

U.S. Environmental Protection Agency. 2002. Urban Stormwater BMP Performance Monitoring: A Guidance Manual for Meeting the National Stormwater BMP Database Requirements. EPA-821-B-02-001. Washington, DC: U.S. Environmental Protection Agency Office of Water.

Walker, W. 1999. Simplified procedures for eutrophication assessment and prediction: User manual. Instruction Report W-96-2. Washington, DC: U.S. Army Corps of Engineers.

Walker, W. 1987. Empirical methods for predicting eutrophication in impoundments: Report 4, phase III: Applications manual. Technical Report E-81-9. Vicksburg, MS: U.S. Army Engineer Waterways Experiment Station.